

Basic Study

Contrast-enhanced micro-computed tomography using ExiTron nano6000 for assessment of liver injury

Xiang-Wei Hua, Tian-Fei Lu, Da-Wei Li, Wei-Gang Wang, Jun Li, Zhen-Ze Liu, Wei-Wei Lin, Jian-Jun Zhang, Qiang Xia

Xiang-Wei Hua, Tian-Fei Lu, Da-Wei Li, Jian-Jun Zhang, Qiang Xia, Department of Liver Surgery and Liver Transplantation Center, Ren Ji Hospital, School of Medicine, Shanghai Jiao Tong University, Shanghai 200127, China

Wei-Gang Wang, Jun Li, Zhen-Ze Liu, Department of Phenotype Analysis, Shanghai Research Center For Model Organisms, Shanghai 200123, China

Wei-Wei Lin, Department of Clinical Laboratory, Ren Ji Hospital, School of Medicine, Shanghai Jiao Tong University, Shanghai 200127, China

Author contributions: All authors contributed to the manuscript.

Supported by National Natural Science Fund, No. 81270558.

Institutional review board statement: The study was reviewed and approved by Ren Ji Hospital, School of Medicine, Shanghai Jiao Tong University Institutional Review Board.

Institutional animal care and use committee: All procedures involving animals were reviewed and approved by the Institutional Animal Care and Use Committee of the Shanghai Jiao Tong University School of Medicine (approval number: SYKX-2008-0050).

Conflict-of-interest statement: The authors declare no conflict of interests.

Data sharing statement: Technical appendix, statistical code, and dataset available from the corresponding author at xiaqiang@shsmu.edu.cn. Participants gave informed consent for data sharing.

Open-Access: This article is an open-access article which was selected by an in-house editor and fully peer-reviewed by external reviewers. It is distributed in accordance with the Creative Commons Attribution Non Commercial (CC BY-NC 4.0) license, which permits others to distribute, remix, adapt, build upon this work non-commercially, and license their derivative works on different terms, provided the original work is properly cited and the use is non-commercial. See: <http://creativecommons.org/licenses/by-nc/4.0/>

[licenses/by-nc/4.0/](http://creativecommons.org/licenses/by-nc/4.0/)

Correspondence to: Qiang Xia, Professor, Department of Liver Surgery and Liver Transplantation Center, Ren Ji Hospital, School of Medicine, Shanghai Jiao Tong University, 1630 Dongfang Road, Pudong New District, Shanghai 200127, China. xiaqiang@shsmu.edu.cn
Telephone: +86-21-68383775
Fax: +86-21-58737232

Received: November 21, 2014

Peer-review started: November 23, 2014

First decision: January 22, 2015

Revised: February 13, 2015

Accepted: March 30, 2015

Article in press: March 31, 2015

Published online: July 14, 2015

Abstract

AIM: To explore the potential of contrast-enhanced computed tomography (CECT) using ExiTron nano6000 for assessment of liver lesions in mouse models.

METHODS: Three mouse models of liver lesions were used: bile duct ligation (BDL), lipopolysaccharide (LPS)/D-galactosamine (D-GalN), and alcohol. After injection with the contrast agent ExiTron nano6000, the mice were scanned with micro-CT. Liver lesions were evaluated using CECT images, hematoxylin and eosin staining, and serum aminotransferase levels. Macrophage distribution in the injury models was shown by immunohistochemical staining of CD68. The *in vitro* studies measured the densities of RAW264.7 under different conditions by CECT.

RESULTS: In the *in vitro* studies, CECT provided specific and strong contrast enhancement of liver in mice. CECT could present heterogeneous images and

densities of injured livers induced by BDL, LPS/D-GalN, and alcohol. The liver histology and immunohistochemistry of CD68 demonstrated that both dilated biliary tracts and necrosis in the injured livers could lead to the heterogeneous distribution of macrophages. The *in vitro* study showed that the RAW264.7 cell masses had higher densities after LPS activation.

CONCLUSION: Micro-CT with the contrast agent ExiTron nano6000 is feasible for detecting various liver lesions by emphasizing the heterogeneous textures and densities of CECT images.

Key words: Micro-computed tomography; ExiTron Nano6000; Liver injury

© The Author(s) 2015. Published by Baishideng Publishing Group Inc. All rights reserved.

Core tip: Noninvasive methods have been extensively studied for examining injuries in small animals in preclinical research. Contrast-enhanced computed tomography (CECT) with ExiTron nano6000 could detect various liver lesions by emphasizing the heterogeneous textures and densities of CECT images. The phenomenon is probably due to the changes in macrophage distribution, number, and function.

Hua XW, Lu TF, Li DW, Wang WG, Li J, Liu ZZ, Lin WW, Zhang JJ, Xia Q. Contrast-enhanced micro-computed tomography using ExiTron nano6000 for assessment of liver injury. *World J Gastroenterol* 2015; 21(26): 8043-8051 Available from: URL: <http://www.wjgnet.com/1007-9327/full/v21/i26/8043.htm> DOI: <http://dx.doi.org/10.3748/wjg.v21.i26.8043>

INTRODUCTION

Small animal models have significantly contributed to the study of liver lesions. Mouse models of liver lesions are frequently limited by difficulties in monitoring disease progression in a longitudinal and noninvasive manner. The assessment of liver lesions during autopsy is time consuming and unfavorable for the principles of animal welfare. Noninvasive methods, including micro-computed tomography (micro-CT), magnetic resonance imaging, positron emission tomography, and ultrasound, have been extensively studied for examining injuries in small animals and are widely used for the diagnosis of organ or tissue damage in clinics^[1-4]. Micro-CT is the best noninvasive method used in preclinical research of animal models because of its excellent spatial resolution^[5]. Initially, micro-CT was implemented in the evaluation of bones, implants and other high-contrast structures because of its poor soft tissue contrast^[6,7]. With the development of contrast agent and X-ray detector sensitivity, micro-CT has been facilitated to enable the

imaging of soft tissues and vessels^[8-11]. Many studies have explored the micro-CT system in the evaluation of liver lesions. Micro-CT was primarily used to detect tumor lesions^[12-14], but recent studies have applied micro-CT to distinguish other types of liver lesions. The degree of liver fibrosis in small animals has been successfully estimated by micro-CT^[15]. Choukèr *et al.*^[16] reported that Contrast-enhanced computed tomography (CECT) with the contrast agent Fenestra VC was available to monitor and localize liver ischemic reperfusion (IR) injury in a murine model. ExiTron nano6000 is a novel liver- and spleen-specific contrast agent that can be administered at a low dosage (100 µL per mouse) and has been shown to be an effective and long-term contrast for detecting liver metastatic tumors^[17,18]. ExiTron nano6000 is primarily taken up by cells in the reticuloendothelial system (RES), including macrophages, which are distributed extensively in the liver as Kupffer cells. Liver lesions could influence the distribution and function of macrophages within the liver. Most studies involving micro-CT have focused on either the imaging of injuries or the characteristics of contrast agents, such as the time course. However, the detailed imaging mechanism has not been discussed. Here, micro-CT with the contrast agent ExiTron nano6000 was applied to assess three types of liver lesions (other than tumor burden): bile duct ligation (BDL), LPS/D-galactosamine (D-GalN), and alcohol. We discuss the related mechanisms of these treatments through the distribution, number, and functional changes of macrophages, which are the major cells that take up ExiTron nano6000.

MATERIALS AND METHODS

Animal care and use

The animal protocol was designed to minimize pain or discomfort to the animals. The animals were acclimatized to laboratory conditions (23 °C, 12 h/12 h light/dark, 50% humidity, *ad libitum* access to food and water) for 2 wk prior to experimentation. Intragastric gavage administration was carried out with conscious animals, using straight gavage needles appropriate for the animal size (15-17 g body weight: 22 gauge, 1 inch length, 1.25 mm ball diameter). All animals were euthanized by pentobarbital (50 mg/kg) for tissue collection.

Animal models

Male C57BL/6 mice (8-10 wk old, weight range 20-25 g) were obtained from the Department of Laboratory Animal Science of Shanghai Jiao Tong University School of Medicine. Induction of cholestatic liver lesions was performed in age-matched male mice (*n* = 5 per group) by ligating the common bile duct (BDL). The mice were anesthetized *via* intraperitoneal injection of pentobarbital (50 mg/kg). After making the abdominal midline incision, the common bile duct

was ligated with 8-0 nylon sutures and transected between the ligatures. The control animals underwent sham operations, whereby the common bile duct was exposed without ligation. Several drops of bupivacaine were applied on the suture line after the muscle layer was closed before closing of the skin wound. These efforts were designed to minimize the suffering of the mice. For fulminant liver lesions, the mice were administered an intraperitoneal injection of D-GalN (700 mg/kg) and *Escherichia coli* lipopolysaccharide (LPS, 10 µg/kg), and the control group received an identical volume of phosphate-buffered saline (PBS) ($n = 5$ per group). For alcohol-induced liver lesions, the mice received one dose of alcohol (5 g/kg body weight, diluted 25:75 vol:vol in water) by gavage ($n = 5$) once daily for four consecutive days. The mice were permitted water and standard pelleted feed during alcohol administration.

Contrast agent and micro-CT images of mice model

ExiTron nano6000 (130-095-146; Miltenyi Biotec) is an alkaline earth metal-based nanoparticulate contrast agent specifically formulated for preclinical CT. It shows strong X-ray absorption due to the high metal load of the particles. Approximately 100 µL of this contrast agent was injected into the tail vein of the mice 4 h before the micro-CT procedure, as previously described, because the density in the liver would reach the highest contrast levels at 4 h after ExiTron nano6000 injection; this effect can last for many days. Upon intravenous injection, ExiTron nano6000 circulates in the bloodstream and is taken up by Kupffer cells (liver macrophages). After ExiTron nano6000 injection, serial micro-CT images of the mice were obtained to observe the macrophage-rich liver. The parameters of the micro-CT scans were as follows: tube voltage: 80 kV; tube current: 0.45 mA; number of views: 400; exposure time: 400 ms; detector bin mode: 2×2 ; and effective pixel size: 0.045 mm. The total scan time was about 20 min for the liver. Analysis of the reconstructed images was performed using Launch GEHC Micro View.

Liver enzyme chemistry and histological analysis

Blood was collected from the retro-orbital sinus to determine the serum alanine aminotransferase (ALT) activity using the Infinity ALT Liquid Stable Reagent (Thermo Fisher Scientific) on a spectrophotometer. The liver tissues were removed from a portion of the left lobe and fixed immediately in 10% neutral-buffered formalin, subsequently dehydrated, and embedded in paraffin. The formalin-fixed and paraffin-embedded tissues were cut serially into 5-µm sections and stained with hematoxylin and eosin (HE). Distribution of the macrophages was detected by immunohistochemistry against CD68 (Gene Tech, Shanghai, China)^[19]. After deparaffinization and rehydration, the sections were soaked in 10 mmol/L citrate buffer (pH 6.0) for antigen retrieval. To block endogenous peroxidase, the sections

were placed in 3% H₂O₂ for 5 min and then washed with PBS. The slides were blocked with 10% normal goat serum for 10 min at 37 °C and incubated overnight at 4 °C with primary antibody. After rinsing with PBS, the sections were incubated with a horseradish-peroxidase-conjugated secondary antibody (Changdao, Shanghai, China) for 30 min at room temperature and then stained with 3,3'-diaminobenzidine (DAB; Maixin-Bio, Guangzhou, China). Hematoxylin was applied for the nuclear staining. Five fields in each liver sample were randomly selected for observation.

Cell culture and micro-CT images of the RAW264.7 cell mass

The murine macrophage cell line RAW264.7, a murine macrophage cell line^[20], was kindly provided by Dr. X. Ma (Key Laboratory of Gastroenterology and Hepatology, Ministry of Health, Shanghai Jiao-Tong University, Shanghai, China). The cells were cultured in DMEM supplemented with 10% FBS, 10 mmol/L L-glutamine, 100 U/mL of penicillin, and 0.1 mg/mL of streptomycin (all purchased from Invitrogen Life Technologies, Carlsbad, CA, United States), at 5% CO₂ and 37 °C. The cells were plated in 60-mm dishes at a density of 0.3×10^6 /mL 1 d before stimulation. The cells were stimulated with 1 µg/mL LPS (Sigma, China) for 12 h followed by co-incubation with ExiTron nano6000 (1:500, vol:vol in DMEM) for 4 h. For the micro-CT images, the cells were washed three times with PBS buffer. Then, the cells were trypsinized and centrifuged at 600 rpm for 5 min to wash out any unendocytosed contrast agent. The cells were resuspended with 1 mL PBS buffer, transferred to 1.5 mL Eppendorf tubes, and centrifuged at 300 g for 5 min. The tubes were held on a foam board and scanned by a micro-CT imaging system with the following parameters: tube voltage, 80 kV; current intensity, 0.45 mA.

Statistical analysis

The probabilities were two-sided and expressed as the mean \pm SD. The data were analyzed with Student's *t* test. We conducted the statistical analysis with SPSS version 19.0 software. We considered values of $P < 0.05$ as statistically significant.

RESULTS

Evaluation of liver lesions with CECT

ExiTron nano6000 as a non-toxic and targeted agent to the liver: The mice showed no observable adverse events or abnormal behavior after injection with ExiTron nano6000^[17]. As shown in Figure 1, ExiTron nano6000 provided specific and strong contrast enhancement of the micro-CT images of the liver and spleen.

CECT images in cholestasis: CECT was first performed on the BDL-treated mice, which are extensively used as

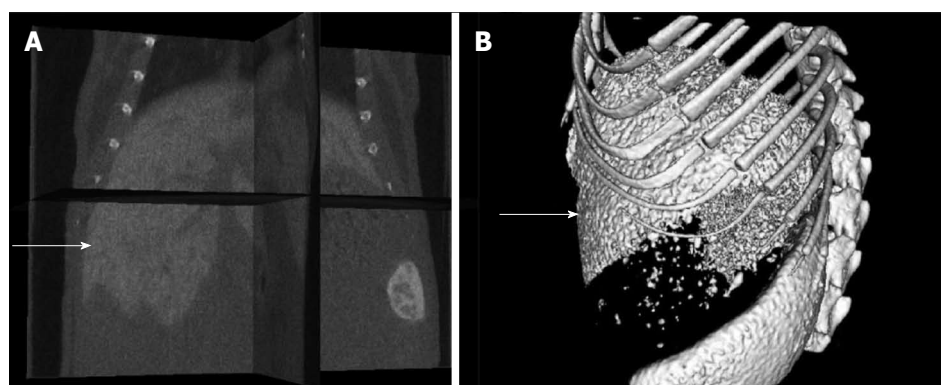


Figure 1 Contrast enhanced computed tomography images of a normal liver. A: 3D image of a liver (arrow); B: Perspective view of a liver (arrow).

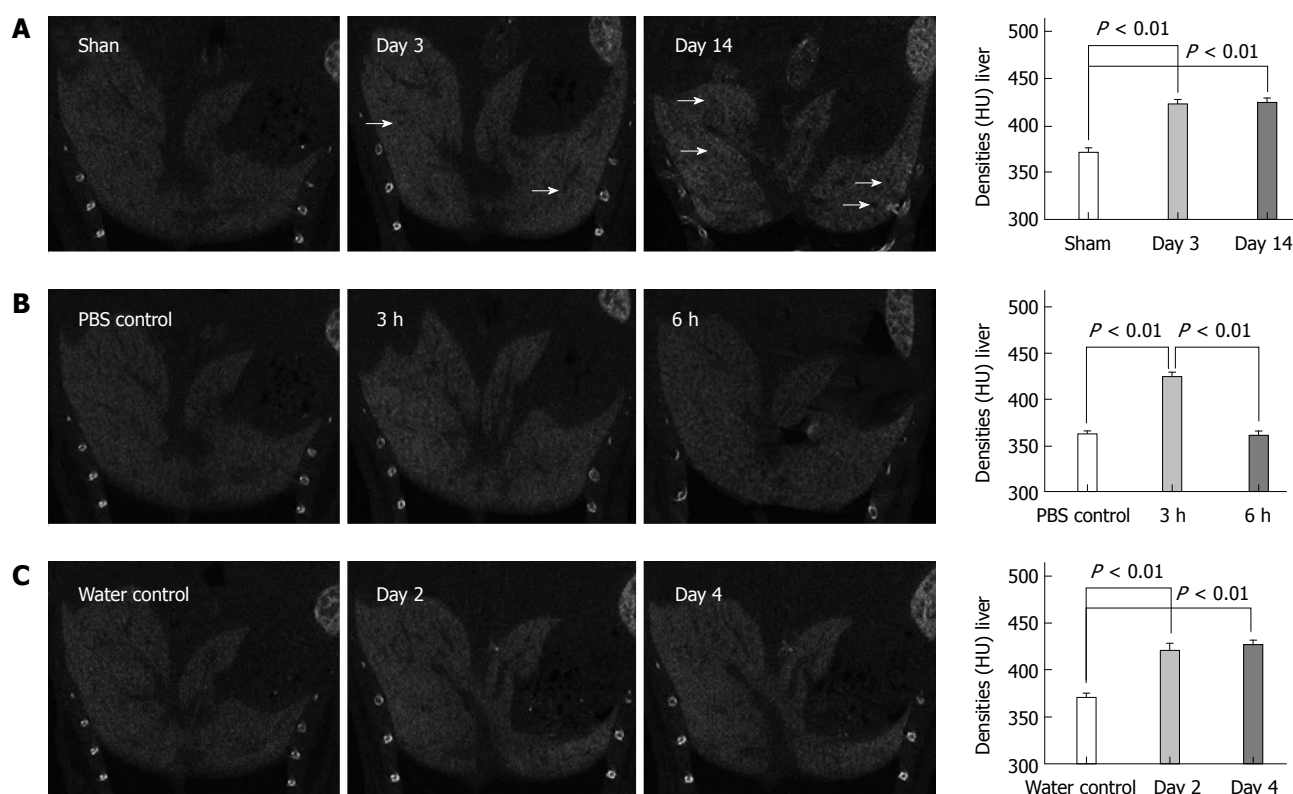


Figure 2 Contrast-enhanced computed tomography images of liver lesions induced by bile duct ligation (A), lipopolysaccharide/D-GalN (B) and alcohol (C); density measured in the livers are reported as HU. The black arrows indicate black regions with low densities. Values are represented as the means of triplicate values and presented as the mean \pm SD.

a cholestasis model. On day 3 after BDL treatment, the texture of the liver became heterogeneous and black regions appeared. The liver density significantly increased compared to that of the sham controls (422.7 ± 7.8 HU vs 374.7 ± 11.4 HU, respectively; $P < 0.001$). On the day 14 after BDL treatment, the texture became more heterogeneous, whereas the black regions became more extensive and larger in the CECT images. Similarly, the liver density was significantly greater compared to that of the sham controls (423.7 ± 8.3 HU vs 367.7 ± 7.8 HU, respectively, $P < 0.001$) (Figure 2A).

CECT applied in LPS/D-GalN and alcohol-induced liver lesions: We performed CECT imaging of LPS/D-GalN-induced liver lesions. The CECT images in Figure 2B show that the texture of the liver became increasingly more heterogeneous, and the black regions became more numerous with the advancement of LPS/D-GalN-induced liver lesions. The liver density showed an up-down trend in that it increased in the early period and decreased in the advanced stages of liver lesions (423.7 ± 8.5 HU for 3 h injury vs 365.0 ± 7.6 HU for PBS control, respectively, $P < 0.001$; 360.7 ± 6.7 HU for 6 h injury vs 360.0 ± 7.2 HU

for PBS control, respectively, $P = 0.91$). For acute alcohol-induced liver lesions, Figure 2C shows that the predominant changes were the increased density of the injured liver compared to that of the sham controls (420.7 ± 11 HU for 2 d injury vs 363.3 ± 8.3 HU for water control, respectively, $P < 0.001$; 426.7 ± 8.0 HU for 4 d injury vs 377.0 ± 9.0 HU for water control, respectively, $P < 0.001$).

Morphological changes influencing the texture of the CECT images: Histology was performed to identify the morphological changes related to the texture of the CECT images, and the serum ALT activities were measured to examine physiologically the extent of the liver lesions. For cholestasis, HE staining showed an increasing bile infarct, dilated biliary tract, and portal liver inflammation with the advancement of cholestasis (Figure 3A). Because ExiTron nano6000 is predominantly taken up by cells of the RES (particularly macrophages within the liver), we studied the effects of liver lesions on the distribution of macrophages in the liver by staining for CD68^[21,22]. This staining showed that macrophages were not present in the area of either the bile infarct or the dilated biliary tract (Figure 3B).

For animals subjected to LPS/D-GalN-induced liver lesions, HE staining primarily showed slight hepatic necrosis accompanying inflammatory cell infiltration at 3 h, and displayed massive necrosis and destruction of the hepatic architecture at 6 h (Figure 3A), which correlated with the serum ALT activities (Figure 4). No macrophages were present in the area of necrosis in CD68-immunostained samples (Figure 3B). For animals subjected to alcohol-induced liver lesions, periportal microvesicular steatosis was observed in the histological examination, and there was no significant change in the distribution of macrophages (Figure 3B).

These results suggest that CECT using ExiTron nano6000 could identify liver lesions such as necrosis and dilated biliary tract by monitoring the distribution of macrophages, which cause various CECT liver textures.

Number and function of macrophages influencing tissue density

Based on the *in vivo* observations described above, we attempted to determine a relationship between the CECT densities of various injured livers and the recruitment of macrophages to the injured livers. Figure 5A shows that the livers from mice subjected to LPS/D-GalN-induced injury for 6 h had significantly fewer macrophages compared to those of the PBS control. Other injuries did not induce any significant changes in the number of macrophages in the livers (Figure 5A), which is consistent with previous studies^[23,24]. We speculated whether liver lesions could improve the endocytotic function of macrophages regarding ExiTron nano6000 uptake and affect the observed increased densities of the injured liver.

We performed CECT of RAW264.7 cells in different states (*i.e.*, quiet or LPS-activated) to confirm the endocytotic ability of macrophages to take up ExiTron nano6000. The results showed that the density of the RAW264.7 cell masses increased significantly after co-incubation with ExiTron nano6000 (135.0 ± 12.8 HU vs -37.00 ± 11.4 HU, respectively, $P < 0.001$). The LPS-activated RAW264.7 cells had a higher density compared to the quiet RAW264.7 cells (184.7 ± 11.0 HU vs 135.0 ± 12.8 HU, respectively, $P < 0.01$) indicating a significant accumulation of ExiTron nano6000 in the LPS-treated RAW264.7 cells (Figure 5B). Besides, hepatocytes were not found to have endocytotic ability when CECT images were performed on the HepG2 cells (data not shown). We concluded that the CECT liver densities were positively correlated with the number and function of macrophages in the liver.

DISCUSSION

Noninvasive detection has become an attractive field in preclinical translational studies^[25-28]. For small animals, a contrast agent is necessary for micro-CT to improve the imaging of soft tissue^[29]. By contrasting macrophages, studies have noninvasively investigated macrophage-rich injuries of soft tissues such as atherosclerotic plaques^[30,31]. Our study has shown that micro-CT using the ExiTron nano6000 contrast agent could detect liver lesions induced by BDL, LPS/D-GalN and alcohol.

Based on the CECT images obtained, ExiTron nano6000 successfully targets and highlights the morphology of the macrophage-rich liver. Extrahepatic cholestasis is a common liver disease and can be caused by diseases including choledocholithiasis and pancreatic disease. BDL-induced liver lesions is a classic model for studying extrahepatic cholestasis and related liver lesions^[32]. In this experiment, CECT showed dark regions that were increased in number and size with the advancement of cholestasis after BDL. Because CECT predominantly shows the areas rich in macrophages (due to ExiTron nano6000 uptake), the dark regions are suggestive of areas that are deficient in macrophages. The increased density of liver after BDL is also an important indication of cholestatic liver lesions.

LPS/D-GalN-induced liver lesions are a useful model for studying fulminant liver failure^[33]. CECT images show a more heterogeneous texture and expanded sporadic black regions with the progression of liver lesions. The liver density in the CECT images significantly increased at 3 h after LPS/D-GalN treatment and then returned to baseline at 6 h. We hypothesize that the enlarged necrotic area accounts for the low density of the liver at 6 h after LPS/D-GalN injection. For the alcohol-induced liver lesions model, the primary change in the CECT images was increased

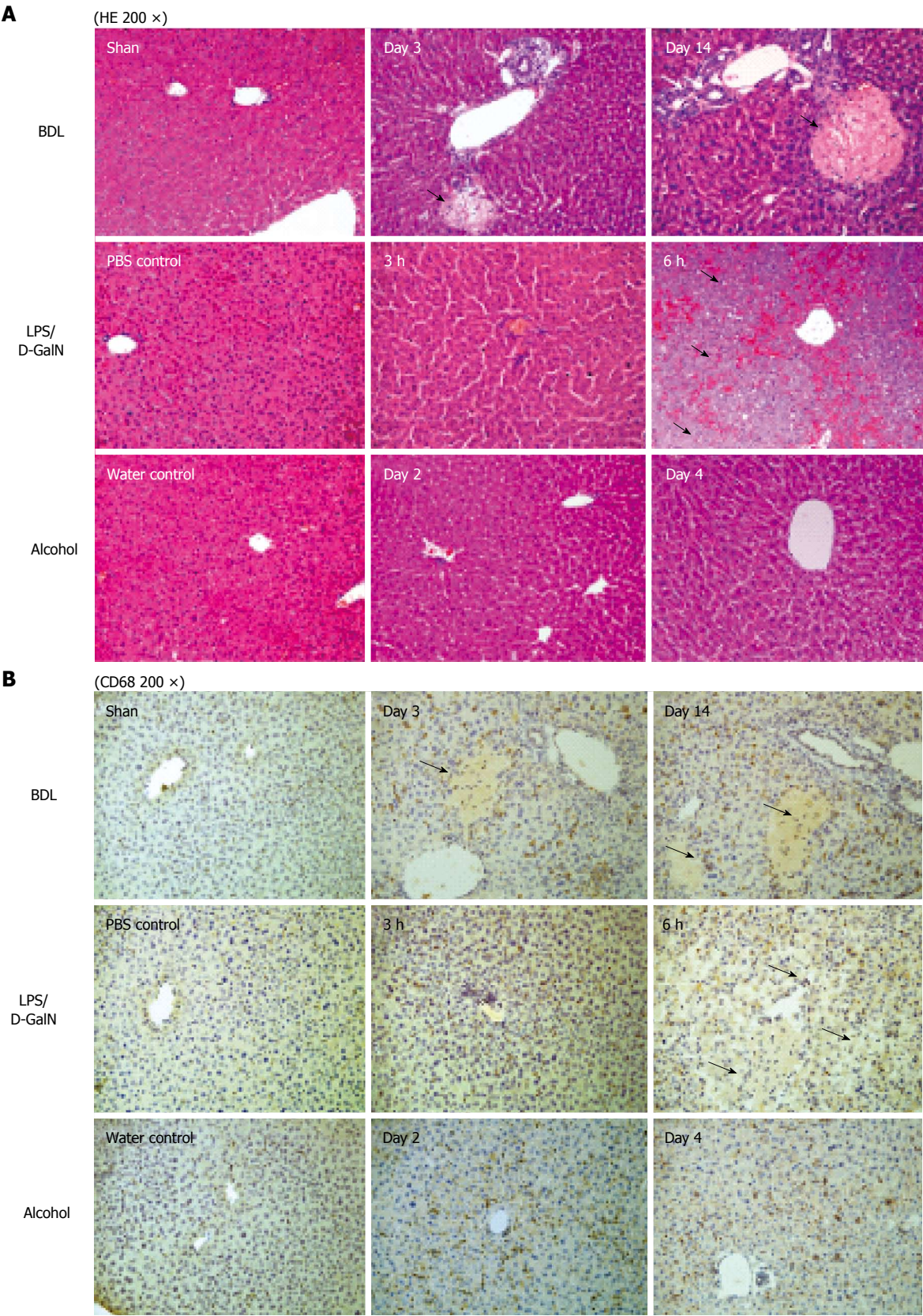


Figure 3 HE stains for liver lesions induced by bile duct ligation, lipopolysaccharide/D-GalN and alcohol (A); Immunostaining of CD68 after liver lesions induced by bile duct ligation, lipopolysaccharide/D-GalN or alcohol (B). The black arrows indicate necrosis, and the white arrows indicate dilated biliary tracts.

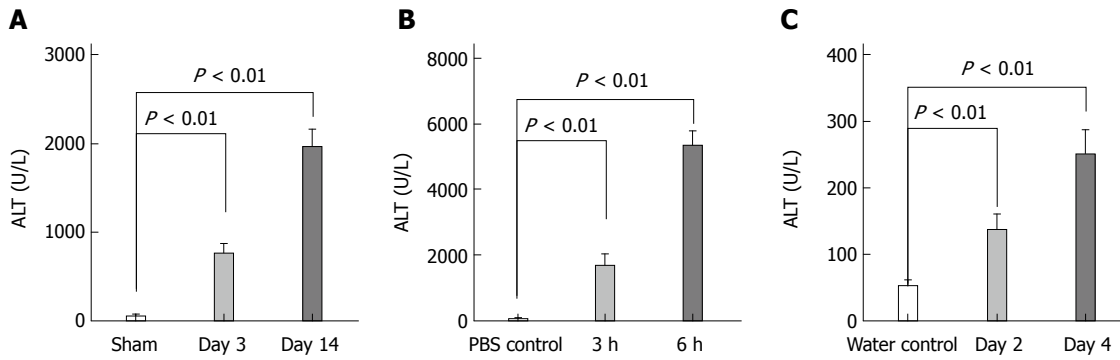


Figure 4 ALT levels in mouse models induced by bile duct ligation (A), lipopolysaccharide/D-GaIN (B) and alcohol (C), ^b $P < 0.01$.

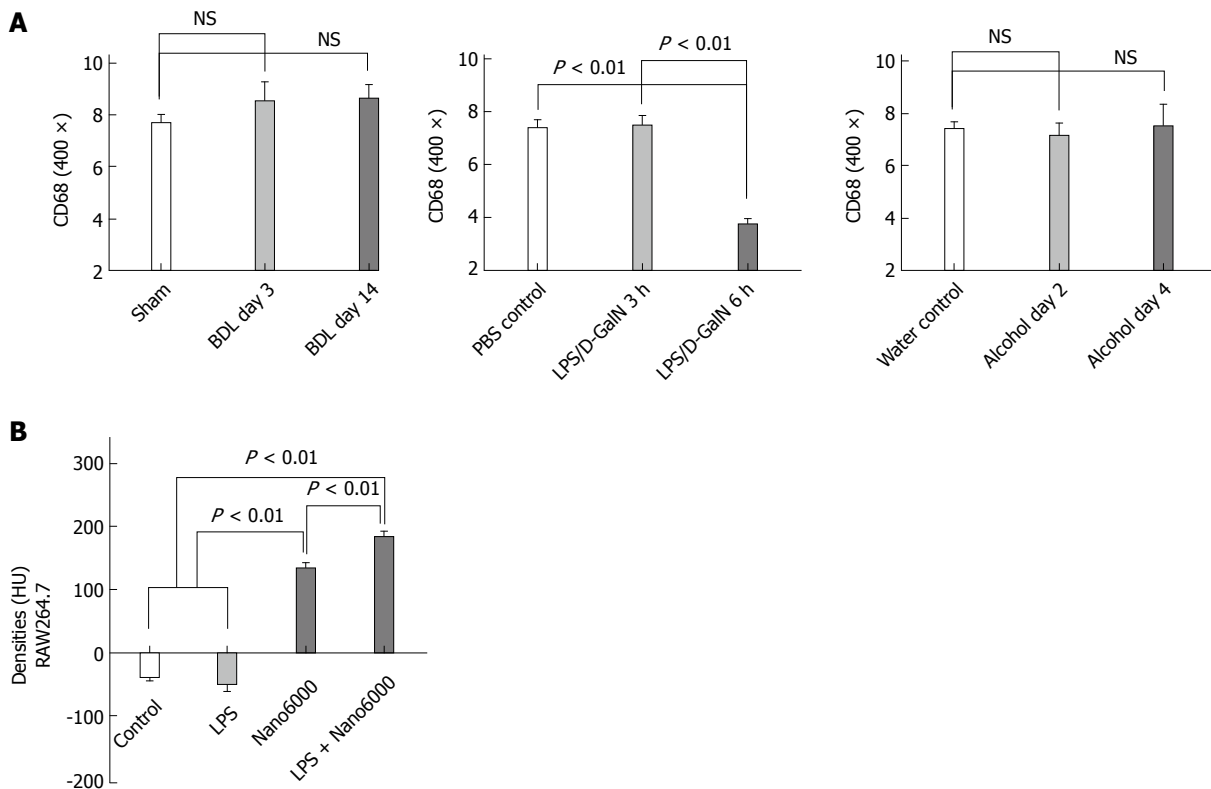


Figure 5 Comparison of the number of CD68+ cells in the injured livers of the three models (A); comparison of the densities of RAW264.7 cell mass co-cultured with nano6000, lipopolysaccharide or both (B). Values are represented as the means of triplicate values and presented as the mean \pm SD.

liver density.

Next, we compared the CECT images and the pathological results, which is the gold standard for the assessment of liver lesions. Comparison demonstrated that the increased density of the CECT images was nearly completely consistent with the pathological results; however, the increased density decreased significantly upon with serious liver lesions such as at 6 h after LPS/D-GaIN injection.

Because the macrophages within the liver represent a major cell type that takes up ExiTron nano6000, we conducted an additional study of the pathology to explore the effect of liver lesions on the distribution and number of macrophages within the liver. By comparing HE and CD68 staining, we determined that various

types of liver lesions could cause the heterogeneous distribution of macrophages instead of changing their numbers. Macrophages were absent in the necrotic area or dilated biliary tract, whereas no significant changes were observed in the healthy regions. By comparing the pathological findings with the CECT images, we concluded that the heterogeneous distribution of macrophages contributed to the heterogeneous texture of the injured livers in the CECT images, and the increased sporadic black regions in the CECT images indicated the areas of either necrosis or dilated biliary tracts.

The unchanged number of macrophages within the injured livers prompted us further to examine changes in macrophage function. The endocytotic ability of

macrophages has been shown to increase significantly after activation^[34]. To understand the relationship between the endocytotic function of macrophages for ExiTron nano6000 and liver lesions, we performed an *in vitro* study using LPS to stimulate RAW246.7 cells^[35,36]. The RAW246.7 cell mass presented a significantly increased density on the CECT images after co-incubation with ExiTron nano6000, which confirmed the ability of macrophages to take up this contrast agent. LPS could activate the Toll-like receptor 4 pathway, which is a classic pathway of macrophage activation in various liver lesions. Consistent with our observations, the LPS-activated RAW246.7 cells had increased densities on the CECT images compared to the nonactivated cells. The results of this *in vitro* study demonstrated that macrophages could be activated by liver lesions and were responsible for the increased density of the injured livers on CECT imaging. These *in vitro* studies suggest that the endocytotic ability of macrophages was activated by liver lesions and resulted in increased density of the injured livers, as observed on CECT imaging.

In conclusion, we demonstrated that micro-CT in conjunction with the ExiTron nano6000 contrast agent could provide specific liver imaging without adverse reactions. CECT was able to detect liver lesions objectively based on the texture and density alterations of the CECT image; these alterations were caused by variations in macrophage distribution, number and function. Besides, ExiTron nano6000 and other contrast agents could also provide pronounced contrast for imaging of adrenal glands, vascular structures or other tissues of interest. All of these suggest that the use of micro-CT could be further expanded in future applications.

COMMENTS

Background

Recently, micro-computed tomography (CT) and many other noninvasive methods have been extensively used to detect liver lesions due to the defects of autopsy, such as being time consuming and unfavorable for the principles of animal welfare. ExiTron nano6000 is an alkaline earth metal-based nanoparticulate contrast agent specifically formulated for preclinical CT. Studies have reported that ExiTron nano6000 could be used to monitor the progress of liver tumor, but liver lesions (other than tumor burden) have not been studied and the detailed imaging mechanism remains to be discussed.

Research frontiers

Micro-CT has been widely used in preclinical small animal studies. Various contrast agents were created to detect the lesions of soft tissues such as blood vessels, brain, liver, and kidney. However, most of them focused on tumor studies. To expand the application of micro-CT are of major interest.

Innovations and breakthroughs

At first, micro-CT using ExiTron nano6000 was successfully implied to detect liver lesions induced by BDL, LPS/D-GalN and alcohol through emphasizing the heterogeneous textures and densities of CECT images. Then, the changes in macrophage distribution, number, and function of liver lesions were found to be the related mechanisms. More importantly, of the mechanisms, we are the first to discuss the role of cellular function in detecting liver lesions by CECT images.

Applications

The study results suggest that micro-CT with the contrast agent ExiTron

nano6000 is a feasible method for detecting various liver lesions.

Terminology

ExiTron nano6000 is an alkaline earth metal-based nanoparticulate contrast agent specifically formulated for preclinical CT. It shows strong X-ray absorption due to the high metal load of the particles. Upon intravenous injection, ExiTron nano6000 circulates in the bloodstream and is primarily taken up by cells in the reticuloendothelial system, including macrophages, which are distributed extensively in the liver as Kupffer cells.

Peer-review

This is a well-done, thoughtful manuscript that is well written. The authors showed that micro-CT with the contrast agent ExiTron nano6000 is potentially useful for detecting various liver lesions such as alcoholic liver changes by the heterogeneous textures and densities images, depending on the distribution, number, and function of macrophages. As a reviewer, I also believe that it has the potential to provide important information about the importance of new technique for detecting different liver lesions.

REFERENCES

- 1 **Deroose CM**, De A, Loening AM, Chow PL, Ray P, Chatziioannou AF, Gambhir SS. Multimodality imaging of tumor xenografts and metastases in mice with combined small-animal PET, small-animal CT, and bioluminescence imaging. *J Nucl Med* 2007; **48**: 295-303 [PMID: 17268028]
- 2 **Wurnig MC**, Tsushima Y, Weiger M, Jungraithmayr W, Boss A. Assessing lung transplantation ischemia-reperfusion injury by microcomputed tomography and ultrashort echo-time magnetic resonance imaging in a mouse model. *Invest Radiol* 2014; **49**: 23-28 [PMID: 24056111 DOI: 10.1097/RLI.0b013e3182a53111]
- 3 **Wu X**, Yu G, Lindner D, Brady-Kalnay SM, Zhang Q, Lu ZR. Peptide targeted high-resolution molecular imaging of prostate cancer with MRI. *Am J Nucl Med Mol Imaging* 2014; **4**: 525-536 [PMID: 25250202]
- 4 **Bastard C**, Bosisio MR, Chabert M, Kalopissis AD, Mahrouf-Yorgov M, Gilgenkrantz H, Mueller S, Sandrin L. Transient micro-elastography: A novel non-invasive approach to measure liver stiffness in mice. *World J Gastroenterol* 2011; **17**: 968-975 [PMID: 21448348 DOI: 10.3748/wjg.v17.i8.968]
- 5 **Martiniova L**, Schimel D, Lai EW, Limpuangthip A, Kvetnansky R, Pacak K. In vivo micro-CT imaging of liver lesions in small animal models. *Methods* 2010; **50**: 20-25 [PMID: 19520168 DOI: 10.1016/j.ymeth.2009.05.016]
- 6 **Borah B**, Dufresne TE, Cockman MD, Gross GJ, Sod EW, Myers WR, Combs KS, Higgins RE, Pierce SA, Stevens ML. Evaluation of changes in trabecular bone architecture and mechanical properties of minipig vertebrae by three-dimensional magnetic resonance microimaging and finite element modeling. *J Bone Miner Res* 2000; **15**: 1786-1797 [PMID: 10976998 DOI: 10.1359/jbmr.2000.15.9.1786]
- 7 **Engelke K**, Graeff W, Meiss L, Hahn M, Delling G. High spatial resolution imaging of bone mineral using computed microtomography. Comparison with microradiography and undecalcified histologic sections. *Invest Radiol* 1993; **28**: 341-349 [PMID: 7683009]
- 8 **Montet X**, Pastor CM, Vallée JP, Becker CD, Geissbuhler A, Morel DR, Meda P. Improved visualization of vessels and hepatic tumors by micro-computed tomography (CT) using iodinated liposomes. *Invest Radiol* 2007; **42**: 652-658 [PMID: 17700281 DOI: 10.1097/RLI.0b013e31805f445b]
- 9 **Ford NL**, Graham KC, Groom AC, Macdonald IC, Chambers AF, Holdsworth DW. Time-course characterization of the computed tomography contrast enhancement of an iodinated blood-pool contrast agent in mice using a volumetric flat-panel equipped computed tomography scanner. *Invest Radiol* 2006; **41**: 384-390 [PMID: 16523021 DOI: 10.1097/01.rli.0000197981.66537.48]
- 10 **Cody DD**, Nelson CL, Bradley WM, Wislez M, Juroske D, Price RE, Zhou X, Bekele BN, Kurie JM. Murine lung tumor measurement using respiratory-gated micro-computed tomography. *Invest Radiol* 2005; **40**: 263-269 [PMID: 15829823]

- 11 **De La Vega JC**, Häfeli UO. Utilization of nanoparticles as X-ray contrast agents for diagnostic imaging applications. *Contrast Media Mol Imaging* 2015; **10**: 81-95 [PMID: 25044541 DOI: 10.1002/cmml.1613]
- 12 **Duan J**, Hu C, Chen H. High-resolution micro-CT for morphologic and quantitative assessment of the sinusoid in human cavernous hemangioma of the liver. *PLoS One* 2013; **8**: e53507 [PMID: 23308240 DOI: 10.1371/journal.pone.0053507]
- 13 **Graham KC**, Detombe SA, MacKenzie LT, Holdsworth DW, MacDonald IC, Chambers AF, Drangova M. Contrast-enhanced microcomputed tomography using intraperitoneal contrast injection for the assessment of tumor-burden in liver metastasis models. *Invest Radiol* 2008; **43**: 488-495 [PMID: 18580331 DOI: 10.1097/RLI.0b013e318172f5b5]
- 14 **Pandit P**, Johnston SM, Qi Y, Story J, Nelson R, Johnson GA. The utility of micro-CT and MRI in the assessment of longitudinal growth of liver metastases in a preclinical model of colon carcinoma. *Acad Radiol* 2013; **20**: 430-439 [PMID: 23498983 DOI: 10.1016/j.acra.2012.09.030]
- 15 **Varenika V**, Fu Y, Maher JJ, Gao D, Kakar S, Cabarrus MC, Yeh BM. Hepatic fibrosis: evaluation with semiquantitative contrast-enhanced CT. *Radiology* 2013; **266**: 151-158 [PMID: 23169796 DOI: 10.1148/radiol.12112452]
- 16 **Choukèr A**, Lizak M, Schimel D, Helmberger T, Ward JM, Despres D, Kaufmann I, Bruns C, Löhe F, Ohta A, Sitkovsky MV, Klauenberg B, Thiel M. Comparison of Fenestra VC Contrast-enhanced computed tomography imaging with gadopentetate dimeglumine and ferucarbotran magnetic resonance imaging for the in vivo evaluation of murine liver damage after ischemia and reperfusion. *Invest Radiol* 2008; **43**: 77-91 [PMID: 18197060 DOI: 10.1097/RLI.0b013e318155aa2e]
- 17 **Boll H**, Nittka S, Doyon F, Neumaier M, Marx A, Kramer M, Groden C, Brockmann MA. Micro-CT based experimental liver imaging using a nanoparticulate contrast agent: a longitudinal study in mice. *PLoS One* 2011; **6**: e25692 [PMID: 21984939 DOI: 10.1371/journal.pone.0025692]
- 18 **Boll H**, Figueiredo G, Fiebig T, Nittka S, Doyon F, Kerl HU, Nölte I, Förster A, Kramer M, Brockmann MA. Comparison of Fenestra LC, ExiTron nano 6000, and ExiTron nano 12000 for micro-CT imaging of liver and spleen in mice. *Acad Radiol* 2013; **20**: 1137-1143 [PMID: 23931428 DOI: 10.1016/j.acra.2013.06.002]
- 19 **You Z**, Wang Q, Bian Z, Liu Y, Han X, Peng Y, Shen L, Chen X, Qiu D, Selmi C, Gershwin ME, Ma X. The immunopathology of liver granulomas in primary biliary cirrhosis. *J Autoimmun* 2012; **39**: 216-221 [PMID: 22727562 DOI: 10.1016/j.jaut.2012.05.022]
- 20 **Venter G**, Oerlemans FT, Wijers M, Willemse M, Fransen JA, Wieringa B. Glucose controls morphodynamics of LPS-stimulated macrophages. *PLoS One* 2014; **9**: e96786 [PMID: 24796786 DOI: 10.1371/journal.pone.0096786]
- 21 **Ishimoto T**, Lanaspá MA, Rivard CJ, Roncal-Jimenez CA, Orlicky DJ, Cicerchi C, McMahan RH, Abdelmalek MF, Rosen HR, Jackman MR, MacLean PS, Diggle CP, Asipu A, Inaba S, Kosugi T, Sato W, Maruyama S, Sánchez-Lozada LG, Sautin YY, Hill JO, Bonthron DT, Johnson RJ. High-fat and high-sucrose (western) diet induces steatohepatitis that is dependent on fructokinase. *Hepatology* 2013; **58**: 1632-1643 [PMID: 23813872 DOI: 10.1002/hep.26594]
- 22 **Benoit B**, Plaisancié P, Awada M, Gélöën A, Estienne M, Capel F, Malpuech-Brugère C, Debard C, Pesenti S, Morio B, Vidal H, Rieusset J, Michalski MC. High-fat diet action on adiposity, inflammation, and insulin sensitivity depends on the control low-fat diet. *Nutr Res* 2013; **33**: 952-960 [PMID: 24176235 DOI: 10.1016/j.nutres.2013.07.017]
- 23 **Barnes MA**, McMullen MR, Roychowdhury S, Pisano SG, Liu X, Stavitsky AB, Bucala R, Nagy LE. Macrophage migration inhibitory factor contributes to ethanol-induced liver injury by mediating cell injury, steatohepatitis, and steatosis. *Hepatology* 2013; **57**: 1980-1991 [PMID: 23174952 DOI: 10.1002/hep.26169]
- 24 **Liu Y**, Ma Z, Zhao C, Wang Y, Wu G, Xiao J, McClain CJ, Li X, Feng W. HIF-1 α and HIF-2 α are critically involved in hypoxia-induced lipid accumulation in hepatocytes through reducing PGC-1 α -mediated fatty acid β -oxidation. *Toxicol Lett* 2014; **226**: 117-123 [PMID: 24503013 DOI: 10.1016/j.toxlet.2014.01.033]
- 25 **Thurman JM**, Rohrer B. Noninvasive detection of complement activation through radiologic imaging. *Adv Exp Med Biol* 2013; **735**: 271-282 [PMID: 23402034]
- 26 **Saito S**, Murase K. Detection and early phase assessment of radiation-induced lung injury in mice using micro-CT. *PLoS One* 2012; **7**: e45960 [PMID: 23029340 DOI: 10.1371/journal.pone.0045960]
- 27 **Wang X**, Hagemeyer CE, Hohmann JD, Leitner E, Armstrong PC, Jia F, Olschewski M, Needles A, Peter K, Ahrens I. Novel single-chain antibody-targeted microbubbles for molecular ultrasound imaging of thrombosis: validation of a unique noninvasive method for rapid and sensitive detection of thrombi and monitoring of success or failure of thrombolysis in mice. *Circulation* 2012; **125**: 3117-3126 [PMID: 22647975 DOI: 10.1161/CIRCULATIONAHA.111.030312]
- 28 **Kuroda H**, Kakisaka K, Kamiyama N, Oikawa T, Onodera M, Sawara K, Oikawa K, Endo R, Takikawa Y, Suzuki K. Non-invasive determination of hepatic steatosis by acoustic structure quantification from ultrasound echo amplitude. *World J Gastroenterol* 2012; **18**: 3889-3895 [PMID: 22876042 DOI: 10.3748/wjg.v18.i29.3889]
- 29 **Hyafil F**, Cornily JC, Feig JE, Gordon R, Vucic E, Amirbekian V, Fisher EA, Fuster V, Feldman LJ, Fayad ZA. Noninvasive detection of macrophages using a nanoparticulate contrast agent for computed tomography. *Nat Med* 2007; **13**: 636-641 [PMID: 17417649 DOI: 10.1038/nm1571]
- 30 **Ding J**, Wang Y, Ma M, Zhang Y, Lu S, Jiang Y, Qi C, Luo S, Dong G, Wen S, An Y, Gu N. CT/fluorescence dual-modal nanoemulsion platform for investigating atherosclerotic plaques. *Biomaterials* 2013; **34**: 209-216 [PMID: 23069709 DOI: 10.1016/j.biomaterials.2012.09.025]
- 31 **Chen W**, Vucic E, Leupold E, Mulder WJ, Cormode DP, Briley-Saebo KC, Barazza A, Fisher EA, Dathe M, Fayad ZA. Incorporation of an apoE-derived lipopeptide in high-density lipoprotein MRI contrast agents for enhanced imaging of macrophages in atherosclerosis. *Contrast Media Mol Imaging* 2008; **3**: 233-242 [PMID: 19072768 DOI: 10.1002/cmml.257]
- 32 **Gujral JS**, Liu J, Farhood A, Jaeschke H. Reduced oncotic necrosis in Fas receptor-deficient C57BL/6J-lpr mice after bile duct ligation. *Hepatology* 2004; **40**: 998-1007 [PMID: 15382126 DOI: 10.1002/hep.20380]
- 33 **Gong X**, Zhang L, Jiang R, Wang CD, Yin XR, Wan JY. Hepatoprotective effects of syringin on fulminant hepatic failure induced by D-galactosamine and lipopolysaccharide in mice. *J Appl Toxicol* 2014; **34**: 265-271 [PMID: 23620140 DOI: 10.1002/jat.2876]
- 34 **May JM**, Huang J, Qu ZC. Macrophage uptake and recycling of ascorbic acid: response to activation by lipopolysaccharide. *Free Radic Biol Med* 2005; **39**: 1449-1459 [PMID: 16274880 DOI: 10.1016/j.freeradbiomed.2005.07.006]
- 35 **Xu X**, Yin P, Wan C, Chong X, Liu M, Cheng P, Chen J, Liu F, Xu J. Punicalagin inhibits inflammation in LPS-induced RAW264.7 macrophages via the suppression of TLR4-mediated MAPKs and NF- κ B activation. *Inflammation* 2014; **37**: 956-965 [PMID: 24473904 DOI: 10.1007/s10753-014-9816-2]
- 36 **Sahin H**, Trautwein C, Wasmuth HE. TLR4 stresses the liver. *Gut* 2012; **61**: 1241-1242 [PMID: 22387524 DOI: 10.1136/gutjnl-2012-302188]

P- Reviewer: Hashimoto N, Homan M, Isaji S

S- Editor: Qi Y L- Editor: Kerr C E- Editor: Liu XM





Published by **Baishideng Publishing Group Inc**

8226 Regency Drive, Pleasanton, CA 94588, USA

Telephone: +1-925-223-8242

Fax: +1-925-223-8243

E-mail: bpgoffice@wjgnet.com

Help Desk: <http://www.wjgnet.com/esps/helpdesk.aspx>

<http://www.wjgnet.com>



ISSN 1007-9327



9 771007 932045